

# High-frequency transport in $p$ -type Si/Si<sub>0.87</sub>Ge<sub>0.13</sub> heterostructures studied with surface acoustic waves in the quantum Hall regime

I. L. Drichko,\* A. M. Diakonov, I. Yu. Smirnov, and G. O. Andrianov

A. F. Ioffe Physico-Technical Institute of Russian Academy of Sciences, 194021 St. Petersburg, Russia

O. A. Mironov, M. Myronov, D. R. Leadley, and T. E. Whall

Department of Physics, University of Warwick, Coventry CV4 7AL, United Kingdom

(Received 16 June 2004; revised manuscript received 1 September 2004; published 26 January 2005)

The interaction of surface acoustic waves (SAWs) with  $p$ -type Si/Si<sub>0.87</sub>Ge<sub>0.13</sub> heterostructures has been studied for SAW frequencies of 30–300 MHz. For temperatures in the range  $0.7 < T < 1.6$  K and magnetic fields up to 7 T, the SAW attenuation coefficient  $\Gamma$  and velocity change  $\Delta V/V$  were found to oscillate with filling factor. Both the real  $\sigma_1$  and imaginary  $\sigma_2$  components of the high-frequency conductivity have been determined and compared with quasi-dc magnetoresistance measurements at temperatures down to 33 mK. By analyzing the ratio of  $\sigma_1$  to  $\sigma_2$ , carrier localization can be followed as a function of temperature and magnetic field. At  $T=0.7$  K, the variations of  $\Gamma$ ,  $\Delta V/V$ , and  $\sigma_1$  with SAW intensity have been studied and can be explained by heating of the two-dimensional hole gas by the SAW electric field. Energy relaxation is found to be dominated by acoustic phonon deformation potential scattering with weak screening.

DOI: 10.1103/PhysRevB.71.045333

PACS number(s): 73.63.Hs, 73.50.Rb

## I. INTRODUCTION

As is well known,<sup>1</sup> in the quantum Hall effect (QHE) regime the magnetic field dependences of the off-diagonal  $\sigma_{xy}^{\text{dc}}$  and diagonal  $\sigma_{xx}^{\text{dc}}$  components of the dc conductivity tensor are very different. Namely,  $\sigma_{xy}^{\text{dc}}$  shows a set of plateaus with abrupt steps taking place at half-integer values of the filling factor  $\nu$ . By contrast,  $\sigma_{xx}^{\text{dc}}$  is extremely small at the quantum Hall plateaux and has sharp maxima at the steps between the plateaux. The conventional explanation is that, at a half-integer filling, electronic states at the Fermi level are extended while at all other filling factors they are localized.

A powerful way to investigate two-dimensional systems, and effectively probe heterostructure parameters, is with a surface acoustic wave (SAW),<sup>2</sup> especially as this is a non-contact measurement: it does not require a Hall bar to be configured and there is no need for carrier injection at the low-dimensional interface. Moreover, simultaneous measurement of the attenuation and velocity of the SAW provides a unique way to determine the complex ac conductivity  $\sigma_{xx}(\omega) = \sigma_1(\omega) - i\sigma_2(\omega)$  as a function of magnetic field, temperature  $T$ , and SAW frequency  $\omega$ . Furthermore, the magnetic field dependence of  $\sigma_{xx}(\omega)$  provides information on both the extended and localized states and allows an analysis of the interplay between these states.<sup>3</sup>

As we observed earlier in GaAs/AlGaAs heterostructures,<sup>4,5</sup> near steps in the Hall conductance, i.e., at half integer  $\nu$ , the imaginary part of the complex ac conductance  $\sigma_2(\omega)$  is small while the real part  $\sigma_1(\omega)$  coincides with the dc transverse conductance  $\sigma_{xx}^{\text{dc}}$ . However, in magnetic fields corresponding to regions near the center of the Hall plateaux, i.e., at small integer  $\nu$ , the difference between  $\sigma_{xx}(\omega)$  and  $\sigma_{xx}^{\text{dc}}$  turns out to be crucial. Namely,  $\sigma_{xx}^{\text{dc}}$  is extremely small while both  $\sigma_1(\omega)$  and  $\sigma_2(\omega)$  are measurable quantities and  $\sigma_2(\omega) \gg \sigma_1(\omega)$ . According to Ref. 6 these facts lead to the conclu-

sion that the mechanism of ac conductance is hopping.

In the present work, for the first time, an acoustic method has been applied in a study of  $p$ -type Si/Si<sub>0.87</sub>Ge<sub>0.13</sub> heterostructures with the purpose of clarifying high-frequency transport mechanisms in the system. Since Ge and Si are not piezoelectric the only way to measure acoustoelectric effects in these structures is via a hybrid method: a SAW propagates along the surface of piezoelectric LiNbO<sub>3</sub> while the Si/SiGe sample is gently pressed onto the LiNbO<sub>3</sub> surface by means of a spring. In this case strain from the SAW is not transmitted to the sample and it is only the electric field accompanying the SAW that penetrates the sample and creates currents that, in turn, produce feedback to the SAW. As a result, both the SAW attenuation coefficient  $\Gamma$  and velocity  $V$  appear to depend on the properties of the two-dimensional hole gas (2DHG). In this paper we present experimental results for SAW frequencies up to 300 MHz, consider localization effects, and analyze the nonlinear SAW interaction with the 2DHG.

## II. EXPERIMENT AND DISCUSSION

In our experimental arrangement the SAW is induced by interdigital transducers at the surface of a piezoelectric LiNbO<sub>3</sub> plate on top of which the sample has been placed. The samples were modulation doped Si/Si<sub>0.87</sub>Ge<sub>0.13</sub> heterostructures with a 2DHG sheet density  $p=2 \times 10^{11}$  cm<sup>-2</sup> and a mobility  $\mu=10\,500$  cm<sup>2</sup>/V s, measured at  $T=4.2$  K. The layered system (shown in Fig. 1) was grown by molecular beam epitaxy at Warwick University starting from a Si(100) substrate, and consisting of an undoped Si buffer layer followed by a 30 nm Si<sub>0.87</sub>Ge<sub>0.13</sub> strained quantum well, a 20 nm undoped spacer and finally a 50 nm boron doped Si layer with an acceptor concentration of  $2.5 \times 10^{18}$  cm<sup>-3</sup>.<sup>7</sup>

Quasi-dc measurements (7–17 Hz) of the resistivity components  $\rho_{xx}$  and  $\rho_{xy}$  have been carried out in magnetic fields

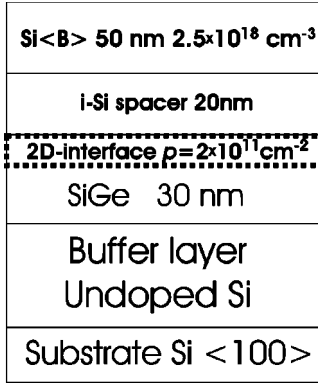
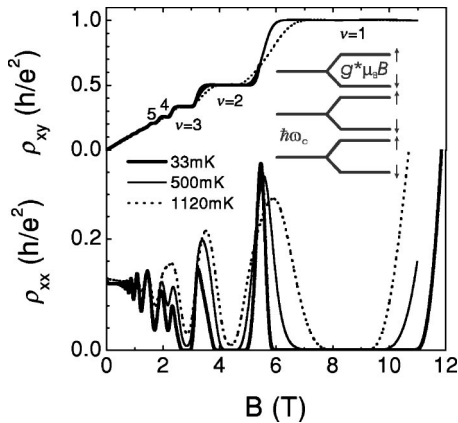
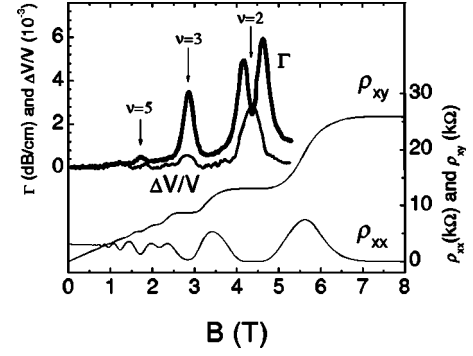


FIG. 1. Layer scheme of the sample.

up to 11 T in the temperature range 33 mK–1.3 K and show the integer quantum Hall effect (Fig. 2). One interesting feature of transport properties in SiGe 2DHGs is the dominance of minima associated with odd filling factors for  $\nu > 2$ . This is because the spin splitting is comparable to the cyclotron energy, with the enhanced exchange interaction increasing the effective  $g$  factor to 4.5,<sup>8–11</sup> and it is illustrated in the inset. As can be seen from Fig. 2, the minima in  $\rho_{xx}$  are more pronounced at  $\nu=3$  and 5 than at  $\nu=4$ , which only appears below 0.5 K. The dc transport measurements were made on a Hall bar sample as electrical contacts were not present on the SAW sample. During the experiments the samples were cooled down several times with only very small differences in conductivity on each cycle, so while the dc conductivity trace does not completely represent that of the sample at the time of SAW investigation we believe it gives a very good indication within experimental uncertainty less than 1%.

The absorption, or attenuation, coefficient  $\Gamma$  and relative velocity change  $\Delta V/V$  of the SAW that interacts with the 2DHG in the SiGe channel, have been simultaneously measured at temperatures  $T=0.7$ –1.6 K in perpendicular magnetic fields up to 7 T. Figure 3 illustrates the field dependence of  $\Gamma$  and  $\Delta V/V$  for a frequency of 30 MHz at 0.7 K together with the magnetoresistance components. One can see that the absorption coefficient and the velocity change both undergo Shubnikov–de Haas (SdH) type oscillations in

FIG. 2. Resistivity components, in units of  $h/e^2$  at different temperatures.FIG. 3. Magnetic field dependence of  $\Gamma$  and  $\Delta V/V$  with a SAW frequency of 30 MHz together with the dc resistivity components  $\rho_{xx}$  and  $\rho_{xy}$ . All at  $T=0.7$  K.

magnetic field, with maxima corresponding to  $\rho_{xx}$  minima and the centers of the IQHE plateaus in  $\rho_{xy}$ , thus allowing the hole density in the 2D channel to be determined directly from acoustic measurements. One exception is the maximum of the attenuation coefficient in the vicinity of  $\nu=2$ , which splits to reveal a minimum in  $\Gamma$  at exactly  $\nu=2$  where the velocity shift is at its largest. This behavior has previously been seen in GaAs samples<sup>2,3</sup> and can be understood through the dependence of  $\Gamma$  on conductivity [see Eqs. (1) and (2) below].

Simultaneous measurements of  $\Gamma$  and  $\Delta V/V$  enable the high-frequency conductivity  $\sigma_{xx}(\omega) = \sigma_1 - i\sigma_2$  to be extracted using the following equations from Ref. 3:

$$\Gamma = 8.68qA(q) \frac{K^2}{2} \frac{\Sigma_1}{\Sigma_1^2 + (1 + \Sigma_2)^2}, \quad \frac{\text{dB}}{\text{cm}}, \quad (1)$$

$$\frac{\Delta V}{V} = A(q) \frac{K^2}{2} \frac{1 + \Sigma_2}{\Sigma_1^2 + (1 + \Sigma_2)^2}, \quad (2)$$

where  $A(q) = 8b(q)(\epsilon_1 + \epsilon_0)\epsilon_s^2\epsilon_0 e^{-2q(a+d)}$  and  $\Sigma_i = (4\pi\sigma_i/\epsilon_s V)t(q)$ ,

$$b(q) = \{b_1(q)[b_2(q) - b_3(q)]\}^{-1},$$

$$t(q) = [b_2(q) - b_3(q)]/2b_1(q),$$

$$b_1(q) = (\epsilon_1 + \epsilon_0)(\epsilon_s + \epsilon_0) - (\epsilon_1 - \epsilon_0)(\epsilon_s - \epsilon_0)e^{-2qa},$$

$$b_2(q) = (\epsilon_1 + \epsilon_0)(\epsilon_s + \epsilon_0) + (\epsilon_1 - \epsilon_0)(\epsilon_s - \epsilon_0)e^{-2qd},$$

$$b_3(q) = (\epsilon_1 - \epsilon_0)(\epsilon_s - \epsilon_0)e^{-2qa} + (\epsilon_1 - \epsilon_0)(\epsilon_s + \epsilon_0)e^{-2q(a+d)}.$$

Here  $K^2$  is the electromechanical coupling constant for lithium niobate (Y cut),  $q$  is the SAW wave vector;  $\epsilon_1=50$ ,  $\epsilon_0=1$ , and  $\epsilon_s=11.7$  are the dielectric constants of  $\text{LiNbO}_3$ , the vacuum and bulk Si, respectively. In these calculations we can ignore the small difference of 4% in dielectric constant between Si and  $\text{Si}_{0.87}\text{Ge}_{0.13}$ . The value of  $d=70$  nm denotes the finite distance between the sample surface and the 2DHG layer and  $a$  is the vacuum clearance between the sample surface and the  $\text{LiNbO}_3$  surface. This clearance remains finite, despite the heterostructure being pressed to the

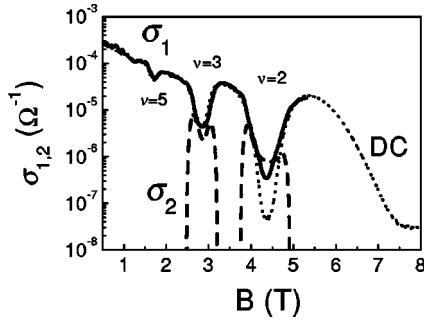


FIG. 4. Magnetic field dependence of  $\sigma_1$  (solid),  $\sigma_2$  (dashed) at  $f=30$  MHz, and  $\sigma_{xx}^{\text{dc}}$  (dotted); all at  $T=0.7$  K.

piezoelectric platelet, because of some roughness of both surfaces. Since the actual clearance is not well controlled, the quantity  $a$  is treated as an adjustable parameter. It is determined by fitting the experimental data at those magnetic fields where the conductance is metallic and essentially frequency independent. In the present experiments the clearance  $a$  ranges from 0.5 to 1.0  $\mu\text{m}$ .<sup>4</sup> Measurements and analysis of the high-frequency conductivity will be considered in two regimes: (A) where the response is linear in applied SAW power and (B) the nonlinear region, when acoustic effects begin to depend on the intensity of the sound wave.

#### A. Linear regime

Figure 4 illustrates the magnetic field dependence of the real  $\sigma_1$  and imaginary  $\sigma_2$  components of the complex high-frequency conductivity, obtained from SAW measurements and using Eqs. (1) and (2), together with the dc conductivity, derived from magnetoresistance measurements via  $\sigma_{xx}^{\text{dc}} = \rho_{xx}/(\rho_{xx}^2 + \rho_{xy}^2)$ , all at  $T=0.7$  K. One can see that  $\sigma_1$  demonstrates SdH-type oscillations and, in the same way as  $\rho_{xx}^{\text{dc}}$ , is dominated by features at odd filling factors—the only minimum at even occupancy is observed at  $\nu=2$ .

It is also evident from Fig. 4 that  $\sigma_1$  is equal to the static conductivity  $\sigma_{xx}^{\text{dc}}$  in the low magnetic field region (below 2 T) and near half-integer filling factors where the electron states are delocalized. However, at magnetic fields close to  $\nu=2$ , where states are strongly localized,  $\sigma_1 \gg \sigma_{xx}^{\text{dc}}$ . Figure 4 also shows that while  $\sigma_2$  is very small near half-integer filling factors and at low magnetic fields, it has appreciable magnitude near to  $\nu=2$  and 3. It is actually double  $\sigma_1$  at  $\nu=2$ , which, along with the fact that  $\sigma_1 \gg \sigma_{xx}^{\text{dc}}$ , points to a manifestation of two-dimensional high-frequency hopping conductivity. It is known that in the IQHE regime carriers can be localized in the random potential generated by charged impurities, with the result that the dc conductivity vanishes and the high-frequency conductivity has to be via hopping. According to Ref. 6, when the 2D high-frequency conductivity has a hopping character, and is determined by hole hops between states close in energy but localized at two different impurity centers (that form pair complexes which do not overlap),  $\sigma_2 \gg \sigma_1$  and  $\sigma_{xx}^{\text{dc}}=0$ . The features we observe at small  $\nu$  thus provide evidence that hole hopping begins to make an important contribution to the high-frequency con-

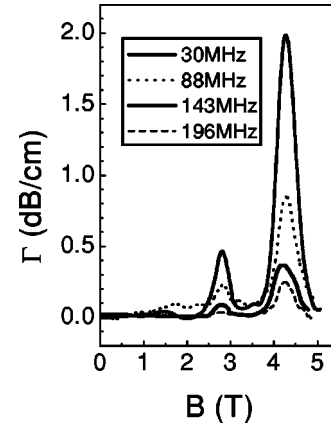


FIG. 5. Magnetic field dependences of the absorption coefficient  $\Gamma$  at different frequencies at  $T=1$  K.

ductivity. However, this would appear not to be the case at lower magnetic fields where  $\sigma_1 = \sigma_{xx}^{\text{dc}}$  and  $\sigma_2$  vanishes. In fact at  $\nu=3$   $\sigma_1 = \sigma_{xx}^{\text{dc}} > \sigma_2$  so even here hopping is not the major high frequency conduction mechanism.

In Ref. 3 it has been shown that for total localization the ratio  $\sigma_2/\sigma_1$  will have the form

$$\frac{\sigma_2}{\sigma_1} = \frac{2\mathcal{L}_\omega(\mathcal{L}_T^2 + \mathcal{L}_T\mathcal{L}_\omega/2 + \mathcal{L}_\omega^2/12) + 4c\mathcal{L}_T^2\mathcal{L}_c}{\pi(\mathcal{L}_T^2 + \mathcal{L}_T\mathcal{L}_\omega + \mathcal{L}_\omega^2/4)}, \quad (3)$$

where  $\mathcal{L}_T = \ln(J/kT)$ , with  $J$  of the order of the Bohr energy,  $\mathcal{L}_\omega = \ln(G_0/\omega)$ ,  $\mathcal{L}_c = \ln(\hbar\omega_c/k_B T)$ , and  $c \geq 1$  is a numerical factor depending on the density of states in the region between the Landau levels. An estimation of  $G_0$  valid for the deformation phonon relaxation mechanism is given in Ref. 12 as  $G_0 = (k_B T)^3 D_{ac}^2 / \rho \hbar^4 s^5$ , where  $D_{ac}$  is the deformation potential,  $\rho$  is the mass density, and  $s$  is the longitudinal sound velocity. Using this estimation one concludes that in the hopping regime  $\sigma_2/\sigma_1 \cong 5$ , whereas experimentally we observe  $\sigma_2/\sigma_1 \cong 2$  in the middle of the  $\nu=2$  Hall plateau. This experimental result suggests that the high-frequency conductivity has a *mixed* mechanism consisting of two contributions: The first we assign to the extended states, while the second, hopping, is associated with the localized states. For  $\nu=3$ , at the lower magnetic field of 2.9 T, the hopping contribution becomes even smaller, and at 1.7 T ( $\nu=5$ ) it is completely absent.

Figure 5 illustrates the effect on the absorption coefficient  $\Gamma$  of varying the SAW frequency at the temperature  $T \cong 1$  K. At this temperature the velocity change  $\Delta V/V$  is small and does not exceed  $3 \times 10^{-4}$  at  $\nu=2$ . Although there are large changes in the magnitude of  $\Gamma$ , these are completely accounted for by the explicitly frequency-dependent factors of Eq. (1). Therefore, within our experimental error, we find no frequency dependence of the acoustically measured conductivity  $\sigma_{xx}(\omega)$  at  $T \cong 1$  K. It is somewhat surprising to see no effect of frequency in the region of  $\nu=2$  where a significant hopping contribution was found at 0.7 K, but we must conclude that the increase in temperature has reduced the relative importance of hopping. Hence, one can see that the acoustic measurements allow an analysis of the  $\sigma_1$  to  $\sigma_2$  ratio

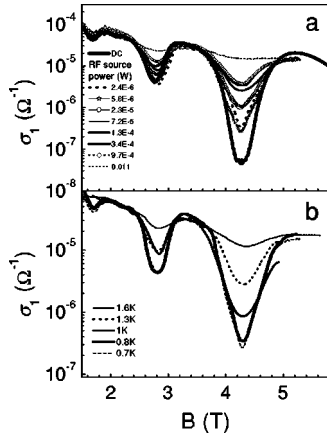


FIG. 6. (a) Dependences of  $\sigma_1$  on magnetic field  $B$  at different rf-source powers,  $T=0.7$ ,  $f=30$  MHz; (b)  $\sigma_1$  versus  $B$  in the linear regime ( $P \approx 5 \times 10^{-6}$  W) at different temperatures,  $f=30$  MHz.

and, thus, the degree of carrier localization can be followed as a function of temperature and magnetic field.

### B. Nonlinear regime

To investigate nonequilibrium effects we have measured the dependence of  $\Gamma$  and  $\Delta V/V$  on the SAW intensity at 30 MHz, by varying the SAW-source power over the range 0.002–11 mW at  $T=0.7$  K. From these measurements  $\sigma_1$  has been extracted and is shown in Fig. 6(a) for the range of rf-source powers. It can be seen that  $\sigma_1$  increases at higher SAW power and we find that the condition  $\sigma_1 \gg \sigma_2$  is satisfied in this nonlinear regime. We interpret this to mean that the high-frequency conductivity is mainly from delocalized holes. These results should be compared with the magnetic field dependence of  $\sigma_1$  extracted from measurements at different temperatures, and sufficiently low power ( $<10^{-5}$  W) to remain in the linear regime, illustrated in Fig. 6(b). For a quantitative comparison, values of  $\sigma_1$  have been taken from Fig. 6 at magnetic fields of 2.9 and 4.3 T, corresponding to  $\nu=3$  and  $\nu=2$ , respectively, and plotted in Fig. 7 as a function of (a) rf-source power  $P$  and (b) temperature. One can see from these plots that  $\sigma_1$  shows similar increases with temperature and SAW power leading to the conclusion that

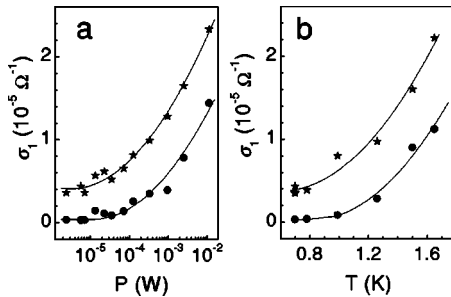


FIG. 7. (a) Dependence of  $\sigma_1$  on the rf-source power  $P$ ; (b) temperature variation of  $\sigma_1$  in the linear regime.  $f=30$  MHz, magnetic fields of 4.3 T (circles) and 2.9 T (stars) correspond to  $\nu=2$  and 3, respectively. The lines are guides to the eye.

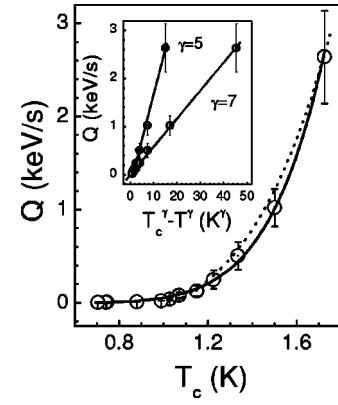


FIG. 8. The energy losses rate per hole measured in acoustics  $Q = \bar{Q}/p$  plotted versus  $T_c$ . Lines are the fitting curves with  $\gamma=5$  (dotted) and  $\gamma=7$  (solid). Inset: dependence of  $Q$  on  $(T_c^\gamma - T^\gamma)$ . Lines are results of the linear fit.

the observed nonlinear effects are probably associated with carrier heating in the SAW electric field.

There have been a number of results published on hole heating by a steady electric field in the 2DHG of Si/SiGe heterostructures.<sup>13–15</sup> However, it is valuable to investigate the energy-loss mechanisms in these structures using a contactless method (such as the possible use of acoustics here) that excludes carrier injection to the low-dimensional interface from contact areas. Hole heating may be described by means of a carrier temperature  $T_c$ , greater than the lattice temperature  $T$ . (The propriety of introducing this carrier temperature will be discussed below.) From Fig. 7,  $T_c$  can be determined by comparing the variation of  $\sigma_1$  on SAW power  $P$  with the curves of  $\sigma_1$  versus the lattice temperature  $T$ , in a manner analogous to SdH thermometry.<sup>16,17</sup> Such a comparison makes it possible to establish a correspondence between the temperature of the 2DHG and the rf-source power.

To characterize the energy relaxation mechanisms one needs to extract the absolute energy loss rate  $\bar{Q}$  resulting from the SAW interaction with the carriers. Since only delocalized states are being considered and  $\sigma_2=0$  we can use the result of Ref. 17 that the energy loss rate is  $\bar{Q} = \sigma_{xx} E^2 = 4\Gamma W$ , where  $E$  is the SAW electric field

$$|E|^2 = K^2 \frac{32\pi}{V} \frac{(\epsilon_1 + \epsilon_0)\epsilon_0^2 q e^{-2q(a+d)}}{b_1^2(q) \{1 + [4\pi\sigma_{xx}(\omega)/(\epsilon_s V) t(q)]^2\}} W, \quad (4)$$

and  $W$  is the input SAW power scaled to the width of the sound track. The resulting energy losses rate per hole  $Q = \bar{Q}/p$  are shown as a function of  $T_c$  in Fig. 8.

From numerous works on dc heating<sup>13–15</sup> a consensus appears that the energy relaxation of holes in Si/SiGe 2DHGs is due to acoustic phonon deformation potential scattering. However, the authors disagree over whether a screened or unscreened deformation potential should be used. The functional form  $Q = A_\gamma (T_c^\gamma - T^\gamma)$ , corresponds to energy relaxation via carrier scattering from the deformation potential of the acoustic phonons with either weak screening ( $\gamma=5$ ) or strong screening ( $\gamma=7$ ) and the slope of inset of Fig. 8 is either<sup>18</sup>

$$A_5 = \frac{3\sqrt{2}m^{*2}\zeta(5)D_{ac}^2k_B^5}{\pi^{5/2}s^4\hbar^7p^{3/2}\rho} \quad (5)$$

or<sup>19–21</sup>

$$A_7 = \frac{45\sqrt{2}m^{*2}\zeta(7)D_{ac}^2k_B^7}{\pi^{5/2}s^6\hbar^9p^{3/2}\rho q_s^2}, \quad (6)$$

where  $m^* = 0.24m_e$  is the effective mass for Si<sub>0.87</sub>Ge<sub>0.13</sub> (Ref. 8) and  $q_s = 2m^*e^2/\epsilon_s\hbar^2 = 7.8 \times 10^6 \text{ cm}^{-1}$  is the screening wave vector for *p*-type SiGe. A least-squares analysis showed that the experimental curves of Fig. 8 could be fitted by the functional form  $Q = A_5(T_c^5 - T^5)$ , but given the small temperature range of the data the form  $Q = A_7(T_c^7 - T^7)$  is equally applicable. In the inset of Fig. 8,  $Q$  is plotted against  $(T_c^\gamma - T^\gamma)$  for both  $\gamma = 5$  and 7 revealing a linear dependence in each case. According to Ref. 22, screening of the hole-phonon interaction can be neglected if the screening wave vector  $q_s$  exceeds the wave vector  $q_e$  of phonons with the average thermal energy, which in our case is  $q_e = 8.2 \times 10^5 \text{ cm}^{-1}$ . Thus,  $q_s \gg q_e$  and the energy relaxation here is dominated unambiguously by unscreened acoustic phonon scattering so we should use  $\gamma = 5$ . This is in agreement with previous work on pseudomorphic Si<sub>1-x</sub>Ge<sub>x</sub> heterostructures with  $x = 0.2$  (Ref. 13) and  $x = 0.15$ ,<sup>15</sup> where weak screening was found to be appropriate for a wide range of hole density up to at least  $10^{12} \text{ cm}^{-2}$ . From the expression for  $A_5$ , the value of the deformation potential can be determined as  $D_{ac} = 5.3 \pm 0.3 \text{ eV}$ . This value is in good agreement with the deformation potential estimate of  $5.5 \pm 0.5 \text{ eV}$  obtained in Ref. 14 for the same SiGe heterostructure from phonon-drag thermopower measurements and, although not agreeing, is of similar magnitude to the values of  $3 \pm 0.4$  and  $2.7 \pm 0.3 \text{ eV}$  reported in Refs. 13 and 15, respectively.

### III. CONCLUSION

For the first time, the contactless acoustic method has been applied to strained *p*-type Si/SiGe heterostructures. Simultaneous measurements of the attenuation and velocity shift of a surface acoustic wave were conducted and used to obtain the high-frequency conductivity and its dependence on magnetic field, temperature, and SAW power. The following conclusions may be drawn from our experimental results and analysis.

In the integer quantum Hall effect regime, the degree of the carrier localization can be followed as a function of magnetic field and/or temperature from the high-frequency conductivity. It is found that even at  $T = 0.7 \text{ K}$  close to the center of the  $\nu = 2$  Hall plateau, only some fraction of the holes in the 2D channel appear to be localized. Thus, the mechanism responsible for the high-frequency conductivity appears to be a mixture of two terms and is determined both by the ex-

tended states as well as hopping via localized states.

In studying nonlinear effects, heating of the 2DHG in Si/SiGe heterostructures by the SAW electric field is observed. This heating could be described by a carrier temperature  $T_c > T$ . From the experimental dependence of the energy loss rate on  $T_c$ , we find that the hole energy relaxation time  $\tau_e$  is determined by dissipation in the unscreened acoustic phonon deformation potential and have obtained values for  $\tau_e$  as well as the deformation potential.

### ACKNOWLEDGMENTS

The work was supported by Grant Nos. RFFI 04-02-16246, NATO-CLG 979355, a Grant of the President of the RF No. NS-2200.2003.2, Prg. of RAN ‘‘Spintronika,’’ and Grant No. INTAS-01-0184.

### APPENDIX: JUSTIFICATION FOR USING $T_c$

The condition for introducing a carrier temperature  $T_c > T$  is that relaxation processes within the carrier gas must be much faster than those leading to thermalization of the carriers, i.e.,

$$\tau_0 \ll \tau_{cc} \ll \tau_e, \quad (A1)$$

where  $\tau_0$ ,  $\tau_{cc}$ , and  $\tau_e$  are the momentum, carrier-carrier, and energy relaxation times, respectively. The momentum relaxation time can be found from the transport mobility as  $\tau_0 = \mu_0 m^*/e = 1.4 \times 10^{-12} \text{ s}$  and is clearly shorter than the carrier-carrier interaction time given by<sup>4,8</sup>

$$\tau_{cc} = \frac{k_B T \rho_{xx} e^2}{2\pi\hbar^2} \ln \frac{h}{2e^2 \rho_{xx}} = 6.4 \times 10^{-11} \text{ s}. \quad (A2)$$

Finally, we can estimate the energy relaxation time  $\tau_e$  from our acoustic measurements. Indeed, if the 2D gas can be characterized by a carrier temperature  $T_c$  and heating is weak  $\Delta T = T_c - T \ll T$ , the energy loss rate per hole can be written in the form<sup>23</sup>  $Q = [\bar{\epsilon}(T_c) - \bar{\epsilon}(T)]/\tau_e$ , where  $\bar{\epsilon}(T_c)$  and  $\bar{\epsilon}(T)$  are the average carrier energy at  $T_c$  and  $T$ , respectively. Assuming also that  $\epsilon_F \gg k_B T$ , the change in average kinetic energy of a hole  $\Delta\epsilon = \bar{\epsilon}(T_c) - \bar{\epsilon}(T)$  is  $\Delta\epsilon = (\pi^2 k_B^2/3) \times (T\Delta T/\epsilon_F)$ . Then, by expanding our previous expression for the loss rate  $Q = A_\gamma(T_c^\gamma - T^\gamma)$  for small  $\Delta T/T$  as  $Q = \gamma A_\gamma T^{\gamma-1} \Delta T$ , we obtain<sup>17</sup>

$$\tau_e = \frac{(\pi k_B)^2}{3\gamma A_\gamma \epsilon_F T^{\gamma-2}}. \quad (A3)$$

Using this equation with  $\gamma = 5$  and finding  $A_\gamma$  from the slope of inset of Fig. 8, we have computed  $\tau_e = (3.8 \pm 0.4) \times 10^{-8} \text{ s}$ . Thus, relation (A1) is satisfied and it is appropriate to introduce a carrier temperature  $T_c$ .

\*Electronic address: irina.l.drichko@mail.ioffe.ru

- <sup>1</sup>R. E. Prange and S. M. Girvin, *The Quantum Hall Effect* (Springer-Verlag, New York, 1987).
- <sup>2</sup>A. Wixforth, J. Scriba, M. Wassermeier, J. P. Kotthaus, G. Weimann, and W. Schlapp, *Phys. Rev. B* **40**, 7874 (1989); R. L. Willett, R. R. Ruel, K. W. West, and L. N. Pfeiffer, *Phys. Rev. Lett.* **71**, 3846 (1993); A. Schenstrom, Y. J. Quian, M. F. Xu, H. P. Baum, H. Levy, and B. K. Sarma, *Solid State Commun.* **65**, 739 (1988).
- <sup>3</sup>I. L. Drichko, A. M. Diakonov, I. Yu. Smirnov, Y. M. Galperin, and A. I. Toropov, *Phys. Rev. B* **62**, 7470 (2000).
- <sup>4</sup>I. L. Drichko, A. M. D'yakonov, A. M. Kreshchuk, T. A. Polyanskaya, I. G. Savel'ev, I. Yu. Smirnov, and A. V. Suslov, *Fiz. Tekh. Poluprovodn. (S.-Peterburg)* **31**, 451 (1997) [*Semiconductors* **31**, 384 (1997)].
- <sup>5</sup>I. L. Drichko, A. M. D'yakonov, V. D. Kagan, I. Yu. Smirnov, and A. I. Toropov, *Proceedings of 24th ICPS*, Jerusalem, edited by D. Gershoni (World Scientific, Singapore, 1998).
- <sup>6</sup>A. L. Efros, *Zh. Eksp. Teor. Fiz.* **89**, 1834 (1985) [*Sov. Phys. JETP* **62**, 1057 (1985)].
- <sup>7</sup>T. E. Whall, N. L. Matthey, A. D. Plews, P. J. Phillips, O. A. Mironov, R. J. Nicholas, and M. J. Kearney, *Appl. Phys. Lett.* **64**, 357 (1994).
- <sup>8</sup>Yu. F. Komnik, V. V. Andrievskii, I. B. Berkutov, S. S. Kryachko, M. Myronov, and T. E. Whall, *Fiz. Nizk. Temp.* **26**, 829 (2000) [*Low Temp. Phys.* **26**, 609 (2000)].
- <sup>9</sup>F. F. Fang, P. J. Wang, B. S. Meyerson, J. J. Nocera, and K. E. Ismail, *Surf. Sci.* **263**, 175 (1992).
- <sup>10</sup>E. Glaser, J. M. Trombetta, T. A. Kennedy, S. M. Prokes, O. J. Glembocki, K. L. Wang, and C. H. Chern, *Phys. Rev. Lett.* **65**, 1247 (1990).
- <sup>11</sup>P. T. Coleridge, A. S. Sachrajda, H. Lafontaine, and Y. Feng, *Phys. Rev. B* **54**, 14 518 (1996).
- <sup>12</sup>Yu. M. Galperin, V. L. Gurevich, and D. A. Parshin, in *Hopping Transport in Solids*, edited by B. Shklovskii and M. Pollak (Elsevier, Amsterdam, 1991).
- <sup>13</sup>G. Ansaripour, G. Braithwaite, M. Myronov, O. A. Mironov, E. H. C. Parker, and T. E. Whall, *Appl. Phys. Lett.* **76**, 1140 (2000).
- <sup>14</sup>S. Agan, O. A. Mironov, M. Tsaousidou, T. E. Whall, E. H. C. Parker, and P. N. Butcher, *Microelectron. Eng.* **51-52**, 527 (2000).
- <sup>15</sup>R. Leturcq, D. L'Hote, R. Tourbot, V. Senz, U. Gennser, T. Ihn, K. Ensslin, G. Dehlinger, and D. Grutzmacher, *Europhys. Lett.* **61**, 499 (2003).
- <sup>16</sup>D. R. Leadley, R. J. Nicholas, J. J. Harris, and C. T. Foxon, *Semicond. Sci. Technol.* **4**, 879 (1989).
- <sup>17</sup>I. L. Drichko, A. M. Diakonov, V. D. Kagan, A. M. Kreshchuk, T. A. Polyanskaya, I. G. Savel'ev, I. Yu. Smirnov, and A. V. Suslov, *Fiz. Tekh. Poluprovodn. (S.-Peterburg)* **31**, 1357 (1997) [*Semiconductors* **31**, 1170 (1997)].
- <sup>18</sup>V. Karpus, *Fiz. Tekh. Poluprovodn. (S.-Peterburg)* **20**, 12 (1986) [*Sov. Phys. Semicond.* **20**, 6 (1986)].
- <sup>19</sup>Y. Ma, R. Fletcher, E. Zaremba, M. D'Iorio, C. T. Foxon, and J. J. Harris, *Phys. Rev. B* **43**, 9033 (1991).
- <sup>20</sup>Peter J. Price, *J. Appl. Phys.* **53**, 6863 (1982).
- <sup>21</sup>R. Fletcher, V. M. Pudalov, Y. Feng, M. Tsaousidou, and P. N. Butcher, *Phys. Rev. B* **56**, 12 422 (1997).
- <sup>22</sup>I. G. Savel'ev, G. Remenyi, Gy. Kovacs, B. Podor, T. A. Polyanskaya, and S. V. Novikov, *Semicond. Sci. Technol.* **14**, 1001 (1999).
- <sup>23</sup>V. F. Gantmakher and I. B. Levinson, *Current Carrier Scattering in Metals and Semiconductors* (Nauka, Moscow, 1984) (in Russian).